Theory of photoluminescence from a magnetic-field-induced two-dimensional quantum Wigner crystal

D. Z. Liu
Center for Superconductivity Research, Department of Physics, University of Maryland, College Park, Maryland 20742

H. A. Fertig
Department of Physics and Astronomy, University of Kentucky, Lexington, Kentucky 40506-0055

S. Das Sarma
Department of Physics, University of Maryland, College Park, Maryland 20742
(Received 10 May 1993)

We develop a theory of photoluminescence using a time-dependent Hartree-Fock approximation that is appropriate for the two-dimensional Wigner crystal in a strong magnetic field. The cases of localized and itinerant holes are both studied. It is found that the photoluminescence spectrum is a weighted measure of the single-particle density of states of the electron system, which for an undisturbed electron lattice has the intricate structure of the Hofstadter butterfly. It is shown that for the case of a localized hole, a strong interaction of the hole with the electron lattice tends to wipe out this structure. In such cases, a single final state is strongly favored in the recombination process, producing a single line in the spectrum. For the case of an itinerant hole, which could be generated in a wide quantum-well system, we find that electron-hole interactions do not significantly alter the density of states of the Wigner crystal, opening the possibility of observing the Hofstadter gap spectrum in the electron density of states directly. At experimentally relevant filling fractions, these gaps are found to be extremely small, due to exchange effects. However, it is found that the hole, which interacts with the periodic potential of the electron crystal, has a Hofstadter spectrum with much larger gaps. It is shown that a finite-temperature experiment would allow direct probing of this gap structure through photoluminescence.

I. INTRODUCTION

The search for a magnetic-field-induced Wigner crystal (WC) in two-dimensional electronic systems has been a subject of long-standing interest. It was first pointed out by Wigner[1] that lowering the density of a quantum electron system would lead to crystallization, since quantum fluctuation effects diminish more rapidly than Coulomb correlation. The relevent comparison is the Coulomb interaction energy $V_c = e^2/\epsilon a$ to the zero-point energy $K = \hbar^2/m^*a^2$, where $a = (\pi n)^{-1/2}$ is the mean interelectron distance and ϵ is the dielectric constant of the host material. Defining the ratio $r_s = V_c/K = a/a_B$, where a_B is the Bohr radius ($= \hbar^2\epsilon/m^*e^2$), crystallization is expected for $r_s \geq 37$ from Monte Carlo simulation results.[2] Wigner crystallization was first experimentally observed in two-dimensional sheets of electrons trapped on the surface of liquid helium,[3] where the electron gas is almost classical. The two-dimensional electron gas (2DEG) in modulation-doped high-mobility GaAs-$Al_xGa_{1-x}As$ heterostructures has proven to be an excellent candidate for observing the formation of a WC in the quantum regime, largely because such high-purity samples are available that the electrons are not necessarily dominated by disorder effect at the low densities required to obtain crystalline order. However, in the absence of a magnetic field, the WC has not been observed in GaAs 2DEG systems.[4] Application of a strong perpendicular magnetic field further enhances the possibility of forming a WC, since this reduces quantum fluctuations (which tend to melt the crystal at large electron density), by confining the electron zero-point motion to cyclotron orbits of radius the magnetic length $l_c = (\hbar c/eB)^{1/2}$. Once l_c is smaller than the mean interelectron distance, Coulomb correlations lead the 2DEG first to form an incompressible liquid phase (fractional quantum Hall effect ground state) at certain densities and ultimately to crystallize below some critical filling factor ν ($= nhc/eB$) $= \nu_c \ll 1$ at low enough temperature. Recent studies of high-mobility heterojunctions in strong magnetic fields have uncovered a number of intriguing properties that in some ways are consistent with the presence of some crystalline order at the lowest available temperatures. These include rf data,[5,6] transport experiments,[7] cyclotron resonance,[8] and photoluminescence (PL) experiments.[9,10] It is the last of these that we will discuss theoretically in this paper.

Photoluminescence experiments on these systems have been performed in two ways. One set of experiments[9] uses a low density of Be dopants that are purposely grown into the sample approximately 250 Å away from the 2DEG. A pulse of light excites a core electron out of a Be^- acceptor, and the photoluminescence spectrum

from recombination of electrons in the 2DEG with the remaining core hole is observed. More recent experiments[10] have also investigated recombination of electrons with itinerant holes in the host crystal (GaAs) valence band. Both experiments show intriguing and complicated results; among them is the observation of a pair of photoluminescence lines that appear at magnetic fields for which transport anomalies recently associated with the WC are found. At the lowest temperatures, the lower of the two lines has most of the oscillator strength; as the temperature is raised, the oscillator strength transfers to the higher of these lines, until the lower line cannot be distinguished from the background. While it is tempting to associate the lower line with a crystal phase, and the upper with a melted phase, the precise interpretation of the data is hampered by a lack of theoretical understanding of what the PL spectrum should look like when the ground state of the 2DEG really is a WC.

To address this problem, we have developed a theory of photoluminescence using a time-dependent Hartree-Fock approximation[11] (TDHFA) that is appropriate for the two-dimensional Wigner crystal in a strong magnetic field. The cases of localized and itinerant holes are both studied. We will show that, within the Hartree-Fock approximation, the photoluminescence spectrum is a weighted measure of the single-particle density of states of the electron system, which for an undisturbed electron lattice has a very interesting structure: for rational filling fractions $\nu = p/q$ there are q subbands, and in Hartree-Fock, p of these are filled. (That the density of states breaks up into q bands in the simultaneous presence of a periodic potential and magnetic field was pointed out by Hofstadter,[12] and this is often referred to as the Hofstadter spectrum.) We therefore expect that for any filling fraction p/q, one should expect to see p lines in the PL for the ideal case of a perfect electron lattice. An observation of this behavior in photoluminescence experiments would yield direct confirmation of the presence of a WC in the system. Unfortunately, we will find that for the case of a localized hole, a strong interaction of the hole with the electron lattice tends to wipe out this structure. In the case of an unscreened hole (e.g., a valence-band hole in a narrow quantum well), this arises because the potential localizes an electron in the vicinity of the hole in the initial state, which dominates the photoluminescence spectrum. For the case of a screened hole, as in a core hole of a neutral acceptor atom, the initial state of the Wigner crystal is relatively undisturbed. However, the only final state which is significantly coupled to via photoluminescence is one in which a vacancy is bound to the charged acceptor ion in the final configuration. In both cases, a single final state is strongly favored in the recombination process, producing a single line in the spectrum. As a function of temperature, we find that this line shifts upward in energy within a very narrow range of the melting temperature. For a system of Wigner crystal domains with a distribution of sizes and melting temperatures, this would appear as a shifting of oscillator strength from a low-energy photoluminescence line to a high-energy one over a range of temperatures. Such behavior is in qualitative agreement with experiment.[10]

For the case of an itinerant hole, which could be generated in a wide-quantum-well system, we find that electron-hole interactions do not significantly alter the density of states of the Wigner crystal. One thus sees, in principle, p lines in the photoluminescence spectrum. Unfortunately, because of the exchange interaction, the gaps between these lines at the relevant small filling fractions may be extremely small, making experimental observation of this effect difficult. We find an interesting possible way out of this difficulty, by considering itinerant holes at finite temperature. For the itinerant case, the hole moves in a periodic potential (of the electron crystal) and a magnetic field, generating a density of states with several bands. Because there is no exchange interaction between the electrons and the hole, we find gaps in the density of states for the latter which are much larger than those of the former. Finite temperature allows a significant probability of occupying some of the higher hole bands in the initial state, leading to several new lines in the photoluminescence spectrum. Once again, observation of this effect would constitute direct confirmation of crystalline order in the 2DEG. We believe that, with improved sample quality, itinerant hole PL experiments should offer the best opportunity to observe this interesting behavior.

This paper is organized in the following way. In Sec. II we show how one can use the TDHFA to compute the photoluminescence spectrum of this system for both localized and itinerant holes. We present and discuss our numerical results in Sec. III. Finally, we summarize our results and make some concluding remarks in Sec. IV. A brief account of some of these results has appeared previously.[13]

II. THEORY

In this section we first present a general expression for the Hartree-Fock Hamiltonian of the 2DEG in a strong magnetic field. We then derive our theory for photoluminescence from a WC in this system within TDHFA for both localized and itinerant holes.

A. Model Hamiltonian

It is well known that noninteracting two-dimensional electrons in a perpendicular magnetic field ($\mathbf{B} = -B\hat{\mathbf{z}}$) have an energy spectrum of discrete Landau levels: $E_N = (N + \frac{1}{2})\hbar\omega_c, N = 0, 1, 2, \ldots$, where $\omega_c = eB/m^*c$ is the cyclotron resonance frequency. Working in the Landau gauge ($\mathbf{A} = -Bx\hat{\mathbf{y}}$), and with periodic boundary conditions in the $\hat{\mathbf{y}}$-direction, the single-particle eigenstates are given by

$$\langle \mathbf{r}|NX\rangle = \frac{1}{L_y}\exp(iXy/l_c^2)\phi_N(x - X). \tag{1}$$

Here $l_c = (\hbar c/eB)^{1/2}$ is the magnetic length and ϕ_N is the one-dimensional harmonic-oscillator eigenstate with oscillation centers X. The allowed values of X are separated by $2\pi l_c^2/L_y$. The degeneracy of each Landau level is given by $g = S/2\pi l_c^2$, with S the area of the 2DEG.

In order to derive the theory of photoluminescence

from a strong-magnetic-field-induced two-dimensional WC, we now consider a system with an interacting 2DEG (within TDHFA) and a layer with a low density of holes (either localized or itinerant) separated by distance d, in the presence of a strong perpendicular magnetic field. Since the magnetic field is very strong, i.e., $\hbar\omega_c \gg e^2/\epsilon a$, and the electronic filling factor $\nu = nhc/eB \ll 1$ in the WC regime, we can assume that only the lowest Landau level is occupied by electrons. The general many-body Hamiltonian can be expressed in terms of single-electron eigenstates (only $N = 0$ eigenstates are included) as follows:

$$\mathcal{H} = \mathcal{H}_0 + \mathcal{H}_{ee} + \mathcal{H}_{eh}, \tag{2}$$

where

$$\mathcal{H}_0 = \sum_X \frac{1}{2}\hbar\omega_c a_X^\dagger a_X + \sum_i E_h c_i^\dagger c_i,$$

$$\mathcal{H}_{ee} = \frac{1}{2S}\sum_{\mathbf{q}} \sum_{X_1X_2X_3X_4} V_c(\mathbf{q})\langle X_1|\exp(i\mathbf{q}\cdot\mathbf{r})|X_4\rangle\langle X_2|\exp(-i\mathbf{q}\cdot\mathbf{r})|X_3\rangle a_{X_1}^\dagger a_{X_2}^\dagger a_{X_3} a_{X_4},$$

$$\mathcal{H}_{eh} = \frac{1}{S}\sum_{\mathbf{q}} \sum_{X_1X_2} \sum_{ij} V_{eh}(\mathbf{q})\langle X_1|\exp(i\mathbf{q}\cdot\mathbf{r})|X_2\rangle\langle i|\exp(-i\mathbf{q}\cdot\mathbf{r})|j\rangle a_{X_1}^\dagger a_{X_2} c_i^\dagger c_j. \tag{3}$$

Here $\mathcal{H}_0$ is the single-particle zero-point energy which is constant. $\mathcal{H}_{ee}$ is the electron-electron interaction, in which $V_c(\mathbf{q}) = 2\pi e^2/\epsilon q$ is the two-dimensional Fourier transform of the Coulomb interaction. $\mathcal{H}_{eh}$ is the electron-hole interaction, in which $V_{eh}(\mathbf{q})$ is the Fourier transform of the interaction between one electron and one hole (for both screened and unscreened hole). In the case of an itinerant hole, the interaction between electron and hole is assumed to be weak enough so that it can be ignored when we calculate the *electronic* density of states. For a system with a small number of holes, it is a good approximation to also ignore hole-hole interactions, which are extremely small in comparison with $\mathcal{H}_{eh}$. In our current consideration, we also do not include the effect of impurities and any external potential. In practice, we may also drop $\mathcal{H}_0$ because it is just a constant. The matrix elements in Eq. (3) are given by

$$\langle X_1|\exp(i\mathbf{q}\cdot\mathbf{r})|X_2\rangle = \exp\left(\frac{i}{2}q_x(X_1+X_2) - \frac{q^2l_c^2}{4}\right) \times \delta_{X_1, X_2+q_y l_c^2}. \tag{4}$$

Shown in Fig. 1 is the electron density profile of a two-dimensional Wigner crystal in a strong magnetic field. Here we assume that the two-dimensional WC is a triangular lattice (which classically is the lowest energy crystal structure at zero temperature).[14] Figure 1(a) illustrates a perfect electronic WC, and Fig. 1(b) is for a WC with one localized hole, at the origin, separated from the plane of the electron gas by a distance d ($\simeq 250$ Å). We can see that the WC deforms around the hole due to the electron-hole interaction. (We will explain below how these figures are derived.) In order to take into account this effect, while still taking advantage of the periodicity of the WC, we divide the WC system into hexagon unit cells. Each supercell contains a finite number of electrons and one hole (in the center, for localized hole case). The

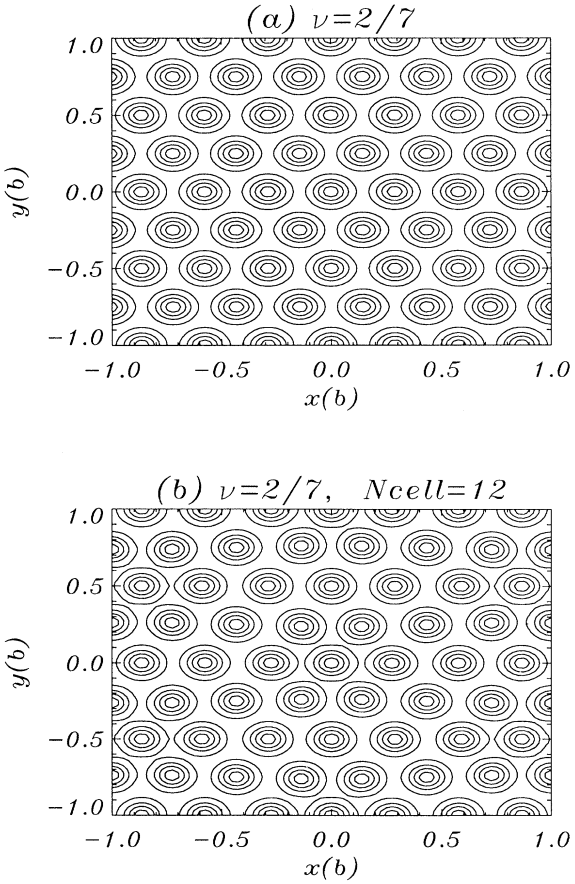

FIG. 1. The density profile for a strong-magnetic-field-induced Wigner crystal at $\nu = 2/7$. (a) For perfect WC with no electron-hole interaction; (b) WC with 12 electrons and one localized hole per supercell in the presence of unscreened electron-hole interaction, where b is the superlattice constant.

finite size of our unit cells will not be significant for large enough supercells.

The density plots illustrated in Fig. 1 were derived using the TDHFA. We briefly review the salient points of the procedure; details may be found in Ref. 15. We first define the density operator

$$n(\mathbf{G}) = \int d^2\mathbf{r} \exp(-i\mathbf{G}\cdot\mathbf{r}) n(\mathbf{r}) = g\rho(\mathbf{G}) \exp\left(-\frac{G^2 l_c^2}{4}\right), \tag{5}$$

where

$$\rho(\mathbf{G}) = \frac{1}{g}\sum_{X_1 X_2} e^{-(i/2)G_x(X_1+X_2)} \delta_{X_1, X_2 - G_y l_c^2} a^\dagger_{X_1} a_{X_2}. \tag{6}$$

One may easily show that

$$\langle \rho(\mathbf{G}=0)\rangle = \frac{\langle N_e\rangle}{g} = \nu. \tag{7}$$

Here N_e is the electron number operator.

The Hartree-Fock Hamiltonian for the 2DEG (with an electron-hole interaction appropriate for a localized hole) in the lowest Landau level can be written as

$$\mathcal{H}_{\rm HF} = g\sum_{\mathbf{G}} \left[W(\mathbf{G})\langle\rho(\mathbf{G})\rangle + n_h V_{eh}(\mathbf{G}) e^{-G^2 l_c^2/4}\right]\rho(\mathbf{G}) \tag{8}$$

where n_h is the density of holes. $W(\mathbf{G})$ is the effective Hartree-Fock interaction

$$W(\mathbf{G}) = \frac{e^2}{\epsilon l_c}\left[\frac{1}{G l_c} e^{-G^2 l_c^2/2}(1-\delta_{\mathbf{G},0}) - \sqrt{\frac{\pi}{2}} e^{-G^2 l_c^2/4} I_0\left(\frac{-G^2 l_c^2}{4}\right)\right] \tag{9}$$

where $I_0(x)$ is the modified Bessel function of the first kind.

B. Green's function, electron density, and density of states

We define single-electron Green's function

$$G(X_1, X_2; \tau) = -\langle T_\tau a_{X_1}(\tau) a^\dagger_{X_2}(0)\rangle. \tag{10}$$

It is convenient to define the Fourier transform

$$G(\mathbf{G},\tau) = \frac{1}{g}\sum_{X_1 X_2} e^{-(i/2)G_x(X_1+X_2)} \times \delta_{X_1, X_2 + G_y l_c^2} G(X_1, X_2; \tau). \tag{11}$$

We will use this form of the Fourier transform throughout this work. The TDHFA is derived by writing the equation of motion for the Green's function,

$$\begin{aligned}\frac{\partial}{\partial\tau} G(X_1, X_2; \tau) &= -\frac{\partial}{\partial\tau}\langle T_\tau a_{X_1}(\tau) a^\dagger_{X_2}(0)\rangle \\ &= -\delta_{X_1 X_2}\delta(\tau) - \langle T_\tau[\mathcal{H} - \mu_e N_e, a_{X_1}](\tau) \\ &\quad \times a^\dagger_{X_2}(0)\rangle.\end{aligned} \tag{12}$$

The commutators may be computed explicitly, and the result is simplified using a Hartree-Fock decomposition. After Fourier transforming with respect to time, the equation of motion for $G(\mathbf{G}, \omega_n)$ can be written as

$$(i\omega_n + \mu_e) G(\mathbf{G}, i\omega_n) - \sum_{\mathbf{G}'} B(\mathbf{G}, \mathbf{G}') G(\mathbf{G}', i\omega_n) = \delta_{\mathbf{G},0}, \tag{13}$$

where

$$\begin{aligned}B(\mathbf{G}_1, \mathbf{G}_2) = [&W(\mathbf{G}_1 - \mathbf{G}_2)\langle\rho(\mathbf{G}_1 - \mathbf{G}_2)\rangle \\ &+ n_h V_{eh}(\mathbf{G}_1 - \mathbf{G}_2) e^{-(\mathbf{G}_1 - \mathbf{G}_2)^2 l_c^2/4}] \\ &\times e^{i(\mathbf{G}_1 \times \mathbf{G}_2) l_c^2/2}.\end{aligned} \tag{14}$$

We can directly diagonalize matrix B and obtain its eigenvectors $V_j(\mathbf{G})$ and eigenvalues ω_j^e, after which the Green's function can be written as

$$\begin{aligned}G(\mathbf{G}, i\omega_n) &= \sum_j \frac{V_j(\mathbf{G}) V_j^*(\mathbf{G}=0)}{i\omega_n + \mu_e - \omega_j^e} \\ &= \sum_j \frac{W_e(\mathbf{G}, j)}{i\omega_n + \mu_e - \omega_j^e}.\end{aligned} \tag{15}$$

The density of states for electrons is then given by

$$\begin{aligned}D(E) &= -\frac{1}{\pi}\mathrm{Im}[G(\mathbf{G}=0, E+i\delta)]\left(\frac{g}{S}\right) \\ &= -\frac{1}{\pi}\mathrm{Im}\left(\sum_j \frac{W_e(\mathbf{G}=0, j)}{E - \omega_j^e + i\delta}\right)\left(\frac{1}{2\pi l_c^2}\right).\end{aligned} \tag{16}$$

Finally, the density operator can be expressed as

$$\begin{aligned}\langle\rho(\mathbf{G})\rangle &= G(\mathbf{G}, \tau = 0^-) \\ &= \sum_j V_j(\mathbf{G}) V_j^*(\mathbf{G}=0) f_{\rm FD}(\omega_j^e - \mu_e).\end{aligned} \tag{17}$$

Here $f_{\rm FD}(x) = [1 + \exp(\beta x)]^{-1}$ is the Fermi-Dirac distribution. Since $\langle\rho(\mathbf{G}=0)\rangle = \nu$, we can self-consistently calculate chemical potential μ_e, the density of states and the electron density in $\mathbf{G}$ space. The density plots in Fig. 1 were obtained by iteratively solving Eqs. (13),(15), and (17).

C. Photoluminescence theory for localized hole

We now present in detail our theory for photoluminescence from the WC in a strong magnetic field. The photoluminescence intensity is given, for a single localized hole state, by

$$P(\omega) = \frac{I_0}{Z}\sum_n \sum_m e^{-E_n/k_B T} |\langle m, 0|\hat{\mathbf{L}}|n, h\rangle|^2 \times \delta(\omega - E_n + E_m), \tag{18}$$

where $Z = \sum_n e^{-E_n/k_BT}$, $|n,h\rangle$ is a many-body electron state with energy E_n and N electrons when there is a core hole present, $|m,0\rangle$ is a many-body electron state with $N-1$ electrons and energy E_m, ω is the luminescence frequency, and $\hat{\mathbf{L}} = \int d^2\mathbf{r}\,\psi(\mathbf{r})\psi_h(\mathbf{r})$ is the luminescence operator, with $\psi(x)$ the electron annihilation operator and $\psi_h(x)$ the hole annihilation operator. As written, the initial state is actually higher in energy than the final state, and we find it convenient to rework the problem in terms of absorption rather than emission. To accomplish this, we add a term $H' = -E_0 c_0^\dagger c_0$ to the Hamiltonian, where $c_0^\dagger$ creates a localized hole, and take the limit $E_0 \to \infty$. It is not difficult to show

$$P(\omega) = \lim_{E_0\to\infty} \frac{P'(\omega - E_0)}{n_0(E_0)} \tag{19}$$

where P' is the absorption spectrum of the new Hamiltonian and n_0 is the average occupation of the hole state, which just becomes one in the limit $E_0 \to \infty$. The absorption spectrum is identical to Eq. (18), except one needs to add the energy E_0 to all the quantities E_n in the expression. After standard manipulations,[16] one can show that

$$P'(\omega) = \frac{I_0}{\pi}\frac{1}{1-e^{\omega/k_BT}}\mathrm{Im}\ R(\omega + i\delta). \tag{20}$$

The function $R(\omega+i\delta)$ is a response function, which continued to imaginary frequency has the form

$$\mathcal{R}(i\omega_n) = -\int_0^\beta \langle T_\tau L(\tau)L^\dagger(0)\rangle e^{i\omega_n\tau}d\tau. \tag{21}$$

To compute this quantity, we consider (for the case of a localized hole state) instead of a single hole, a periodic (hexagonal) lattice of them, with a unit cell that contains as many electrons as can be handled numerically. We allow neither interactions between the holes nor tunneling between the hole sites, so that in the limit of large unit (super)cells, one should expect the result to be the same as for the isolated hole case.

The quantity of interest arising out of Eq. (21) is

$$\mathcal{R}_{ij}(X_1,X_2;\tau) = -\langle T_\tau a_{X_1}(\tau)c_i(\tau)c_j^\dagger(0)a_{X_2}^\dagger(0)\rangle. \tag{22}$$

We write down the equation of motion for $\mathcal{R}_{ij}(X_1,X_2;\tau)$ in terms of its commutator with the Hamiltonian:

$$\begin{aligned}\frac{\partial}{\partial\tau}\mathcal{R}_{ij}(X_1,X_2;\tau) &\equiv -\frac{\partial}{\partial\tau}\langle T_\tau a_{X_1}(\tau)c_i(\tau)c_j^\dagger(0)a_{X_2}^\dagger(0)\rangle \\ &= -\langle[a_{X_1}c_i, c_j^\dagger a_{X_2}^\dagger]\rangle\delta(\tau) - \langle T_\tau[\mathcal{H}_{\mathrm{eff}} - \mu(N_e-N_h), a_{X_1}c_i](\tau)c_j^\dagger a_{X_2}^\dagger\rangle,\end{aligned} \tag{23}$$

where $\mathcal{H}_{\mathrm{eff}} = \mathcal{H} - E_0\sum_i c_i c_i^\dagger$ and N_e and N_h are corresponding electron and hole number operator. Here

$$\begin{aligned}\mathcal{H}_T &= \mathcal{H}_{\mathrm{eff}} - \mu(N_e - N_h) \\ &= \mathcal{H}_0 + \mathcal{H}_{ee} + \mathcal{H}_{eh} - E_0\sum_i c_i c_i^\dagger - \mu(N_e - N_h) \\ &= H_1 + H_2 + H_3,\end{aligned} \tag{24}$$

where

$$\begin{aligned}H_1 &= (\tfrac{1}{2}\hbar\omega_c - \mu)\sum_X a_X^\dagger a_X + (E_h - E_0 + \mu)\sum_i c_i^\dagger c_i, \\ H_2 &= \mathcal{H}_{ee}, \\ H_3 &= \mathcal{H}_{eh}.\end{aligned} \tag{25}$$

We can thus write Eq. (23) as

$$\frac{\partial}{\partial\tau}\mathcal{R}_{ij}(X_1,X_2;\tau) = -T_0 - T_1 - T_2 - T_3, \tag{26}$$

where T_0 is the first term on the right-hand side of Eq. (23) and the T_i's represent the commutator terms with each of the H_i's.

In the limit $E_0 \to \infty$, the first term can be written as

$$\begin{aligned}T_0 &= [\langle a_{X_1}a_{X_2}^\dagger\rangle\delta_{ij} - \langle c_j^\dagger c_i\rangle\delta_{X_1X_2}]\delta(\tau) \\ &= \lim_{n_0\to 1}[\langle a_{X_1}a_{X_2}^\dagger\rangle - n_0\delta_{X_1X_2}]\delta_{ij}\delta(\tau) \\ &= -\langle a_{X_2}^\dagger a_{X_1}\rangle\delta_{ij}\delta(\tau).\end{aligned} \tag{27}$$

Its Fourier transformation is

$$\begin{aligned}\widetilde{T}_0(\mathbf{G},\tau) &= \frac{1}{g}\sum_{X_1X_2} e^{-(i/2)G_x(X_1+X_2)}\delta_{X_2,X_1-G_yl_c^2}T_0 \\ &= -\langle\rho(\mathbf{G})\rangle\delta_{ij}\delta(\tau).\end{aligned} \tag{28}$$

Since H_1 essentially provides a constant energy shift to the system, the second term can be easily calculated:

$$\begin{aligned}T_1 &= \langle T_\tau[H_1, a_{X_1}c_i](\tau)c_j^\dagger a_{X_2}^\dagger\rangle \\ &= (\tfrac{1}{2}\hbar\omega_c + E_h - E_0)\mathcal{R}_{ij}(X_1,X_2;\tau)\end{aligned} \tag{29}$$

so that

$$\widetilde{T}_1(\mathbf{G},\tau) = (\tfrac{1}{2}\hbar\omega_c + E_h - E_0)\mathcal{R}_{ij}(\mathbf{G},\tau). \tag{30}$$

In order to calculate the third term (contribution of electron-electron interaction), we first compute the commutator and then apply a Hartree-Fock decomposition technique[15] to get

$$\begin{aligned}T_2(X,X';\tau) &= \langle T_\tau[H_2, a_X c_i](\tau)c_j^\dagger a_{X'}^\dagger\rangle \\ &= \frac{1}{S}\sum_{\mathbf{q}}\sum_{X_1X_2X_3X_4} V_c(\mathbf{q})\langle X_1|\exp(i\mathbf{q}\cdot\mathbf{r})|X_4\rangle\langle X_2|\exp(-i\mathbf{q}\cdot\mathbf{r})|X_3\rangle \\ &\quad\times\{\langle a_{X_1}^\dagger a_{X_4}\rangle\delta_{XX_2}\mathcal{R}_{ij}(X_3,X';\tau) - \langle a_{X_1}^\dagger a_{X_3}\rangle\delta_{XX_2}\mathcal{R}_{ij}(X_4,X';\tau)\}.\end{aligned} \tag{31}$$

Substituting

$$\langle a^{\dagger}_{X_1} a_{X_2}\rangle = \sum_{\mathbf{G}} \langle \rho(\mathbf{G})\rangle e^{(i/2)G_x(X_1+X_2)}\delta_{X_1,X_2-G_y l_c^2}, \tag{32}$$

and Eq. (4), after some lengthy algebra, we obtain the final expression

$$T_2(X,X';\tau) = \sum_{\mathbf{G}} W(\mathbf{G})\langle \rho(\mathbf{G})\rangle e^{iG_x(X-G_y l_c^2/2)}\mathcal{R}_{ij}(X - G_y l_c^2, X';\tau). \tag{33}$$

Its Fourier transform can be written as

$$\widetilde{T}_2(\mathbf{G},\tau) = \sum_{\mathbf{G}'} W(\mathbf{G}')\langle \rho(\mathbf{G}')\rangle e^{-i(\mathbf{G}\times\mathbf{G}')l_c^2/2}\mathcal{R}_{ij}(\mathbf{G}-\mathbf{G}',\tau). \tag{34}$$

Now we turn to the fourth term (contribution from electron-hole interaction). We apply the same Hartree-Fock decomposition technique and obtain

$$\begin{aligned} T_3 &= \langle T_\tau[H_3, a_X c_i](\tau) c_j^{\dagger} a^{\dagger}_{X'}\rangle \\ &= \frac{1}{S}\sum_{\mathbf{q}}\sum_{X_1X_2} V_{eh}(\mathbf{q})\langle X_1|\exp(i\mathbf{q}\cdot\mathbf{r})|X_2\rangle \Bigg\{ \langle a^{\dagger}_{X_1}a_{X_2}\rangle e^{-i\mathbf{q}\cdot\mathbf{R}_i}\mathcal{R}_{ij}(X,X') \\ &\quad + \left[n_0 N_c \sum_{\mathbf{G}} \delta_{\mathbf{q},\mathbf{G}}\delta_{X_1X} + (1-n_0)\delta_{X_1X}e^{-i\mathbf{q}\cdot\mathbf{R}_i} - \langle a^{\dagger}_{X_1}a_X\rangle e^{-i\mathbf{q}\cdot\mathbf{R}_i}\right]\mathcal{R}_{ij}(X_2,X')\Bigg\} \end{aligned} \tag{35}$$

where N_c is the total number of supercells. In deriving the above equation, we assume there is no overlap between hole states (i.e., single-hole approximation), so

$$\langle i|\exp(-i\mathbf{q}\cdot\mathbf{r})|j\rangle = \exp(-i\mathbf{q}\cdot\mathbf{R}_i)\delta_{ij} \tag{36}$$

where $\mathbf{R}_i$ is the hole (or supercell) superlattice vector. We then substitute Eqs. (32) and (4) into Eq. (35) and take $n_0 = 1$, and after a very involved calculation, we get

$$\begin{aligned} T_3(X,X';\tau) = \sum_{\mathbf{q}} V_{eh}(\mathbf{q}) e^{-q^2 l_c^2/4 - iq_x q_y l_c^2/2} \\ \times \Bigg[\frac{1}{2\pi l_c^2}\sum_{\mathbf{G}}\langle\rho(\mathbf{G})\rangle\delta_{\mathbf{q},-\mathbf{G}} e^{iG_xG_y l_c^2/2}\mathcal{R}_{ij}(X,X') + n_h\sum_{\mathbf{G}}\delta_{\mathbf{q},\mathbf{G}}e^{iq_xX}\mathcal{R}_{ij}(X - q_y l_c^2, X') \\ - \frac{1}{S}\sum_{\mathbf{G}}\langle\rho(\mathbf{G})\rangle e^{-i\mathbf{q}\cdot\mathbf{R}_i}e^{iq_x(X-G_y l_c^2)+iG_x(X-G_y l_c^2/2)}\mathcal{R}_{ij}[X-(q_y+G_y)l_c^2, X']\Bigg] \end{aligned} \tag{37}$$

in which the last term[17] can be dropped as we take the limit $S\to\infty$. Its Fourier transformation can be written as

$$\widetilde{T}_3(\mathbf{G},\tau) = \frac{1}{2\pi l_c^2}\sum_{\mathbf{G}'} V_{eh}(-\mathbf{G}')\langle\rho(\mathbf{G}')\rangle e^{-G'^2 l_c^2/4}\mathcal{R}_{ij}(\mathbf{G},\tau) + n_h\sum_{\mathbf{G}'} V_{eh}(\mathbf{G}')e^{-G'^2 l_c^2/4 - i(\mathbf{G}\times\mathbf{G}')l_c^2/2}\mathcal{R}_{ij}(\mathbf{G}-\mathbf{G}',\tau). \tag{38}$$

So finally, in the $\mathbf{G}$ space, equation of motion for $\mathcal{R}_{ij}$ is

$$\frac{\partial}{\partial\tau}\mathcal{R}_{ij}(\mathbf{G},\tau) = -\widetilde{T}_0 - \widetilde{T}_1 - \widetilde{T}_2 - \widetilde{T}_3. \tag{39}$$

When transformed into real frequency space, it becomes

$$\begin{aligned} -(\omega+i\delta)R_{ij}(\mathbf{G},\omega) &= \langle\rho(\mathbf{G})\rangle\delta_{ij} + (E_0 - \tfrac{1}{2}\hbar\omega_c - E_h)R_{ij}(\mathbf{G},\omega) \\ &\quad - \sum_{\mathbf{G}'} W(\mathbf{G}')\langle\rho(\mathbf{G}')\rangle e^{-i(\mathbf{G}\times\mathbf{G}')l_c^2/2}R_{ij}(\mathbf{G}-\mathbf{G}',\omega) \\ &\quad - \frac{1}{2\pi l_c^2}\sum_{\mathbf{G}'} V_{eh}(-\mathbf{G}')\langle\rho(\mathbf{G}')\rangle e^{-G'^2 l_c^2/4}R_{ij}(\mathbf{G},\omega) \\ &\quad - n_h\sum_{\mathbf{G}'} V_{eh}(\mathbf{G}')e^{-G'^2 l_c^2/4 - i(\mathbf{G}\times\mathbf{G}')l_c^2/2}R_{ij}(\mathbf{G}-\mathbf{G}',\omega). \end{aligned} \tag{40}$$

It is apparent that the solution to this satisfies

$$R_{ij}(\mathbf{G},\omega) = R(\mathbf{G},\omega)\delta_{ij}. \tag{41}$$

This result may be expressed in the form

$$\sum_{\mathbf{G}'}[(\omega + i\delta + E_0 - \omega_0)\delta_{\mathbf{G},\mathbf{G}'} - B(\mathbf{G},\mathbf{G}')]R(\mathbf{G}',\omega) = -\langle\rho(\mathbf{G})\rangle, \tag{42}$$

where

$$\omega_0 = \frac{1}{2}\hbar\omega_c + E_h + \frac{1}{2\pi l_c^2}\sum_{\mathbf{G}}\langle\rho(\mathbf{G})\rangle V_{eh}(-\mathbf{G})e^{-G^2l_c^2/4}, \tag{43}$$

and B is exactly given by Eq. (14). Finally, it is not difficult to show that

$$R(\omega) = \frac{n_h S}{2\pi l_c^2}\sum_{\mathbf{G}} R(\mathbf{G},\omega)e^{-G^2l_c^2/4}, \tag{44}$$

and the PL spectrum may now be computed using Eqs. (19) and (20).

We see that the form of R is essentially that of electron Green's function as in Eq. (13). By inverting Eq. (42), we have

$$\begin{aligned} R(\mathbf{G},\omega) &= -\sum_{\mathbf{G}'}[(\omega + i\delta + E_0 - \omega_0)\delta_{\mathbf{G},\mathbf{G}'} \\ &\quad - B(\mathbf{G},\mathbf{G}')]^{-1}\langle\rho(\mathbf{G}')\rangle \\ &= -\sum_{j\mathbf{G}'}\frac{V_j(\mathbf{G})V_j^{-1}(\mathbf{G}')\langle\rho(\mathbf{G}')\rangle}{\omega + i\delta - \omega_0 - \omega_j^e} \qquad (45) \\ &= -\sum_{j}\frac{W_e(\mathbf{G},j)f_{\mathrm{FD}}(\omega_j^e - \mu_e)}{\omega + i\delta - \omega_0 - \omega_j^e}. \qquad (46) \end{aligned}$$

Here we have already dropped E_0 because it cancels out when we calculate the final photoluminescence power using Eqs. (19) and (20). We can see that R has poles at precisely the same energies as the poles in the electron Green's function for the system in the presence of the external interaction V_{eh} due to the hole,[18] up to the constant energy shift ω_0.[19,20] Thus, the photoluminescence spectrum is indeed a weighted measure of the single-particle density of states of the electron system with a localized hole.

D. Photoluminescence theory for itinerant hole

The case of the itinerant hole is treated similarly to the case outlined above, except that there is an important simplification: since the hole density is low at all points in space, it is safe to ignore any deformation of the electron lattice due to the hole. Since the itinerant hole is moving (in a layer a distance d away from the electron layer) in the periodic potential of the electron lattice, there will be many hole states forming several bands similar to the density of states of the electronic Wigner crystal. For simplicity, we work in the lowest Landau level of the hole, although in real systems the relatively heavy hole mass would allow some (possibly significant) Landau level mixing. Ignoring this, however, should not affect our qualitative conclusions. We can define single-particle Green's function for the itinerant hole:

$$G_h(X_1,X_2) = -\langle T_\tau c_{X_1}(\tau)c_{X_2}^\dagger(0)\rangle. \tag{47}$$

We can also use TDHFA to derive the equation of motion for itinerant hole Green's function. In the momentum space, $G_h^*(\mathbf{G},\omega_n)$ satisfies

$$(i\omega_n + \mu_h)G_h^*(\mathbf{G},\omega_n) - \sum_{\mathbf{G}'}B_h(\mathbf{G},\mathbf{G}')G_h^*(\mathbf{G}',\omega_n) = \delta_{\mathbf{G},0}, \tag{48}$$

where

$$B_h(\mathbf{G},\mathbf{G}') = -\frac{e^2}{\epsilon l_c}\frac{1}{Gl_c}(1-\delta_{\mathbf{G},0})e^{-Gd-G^2l_c^2/2+i(\mathbf{G}\times\mathbf{G}')l_c^2/2} \times\langle\rho(\mathbf{G})\rangle. \tag{49}$$

We solve the eigenvalue problem

$$\sum_{\mathbf{G}'}B_h(\mathbf{G},\mathbf{G}')V_h(\mathbf{G}',j) = \omega_j^h V_h(\mathbf{G},j), \tag{50}$$

so that

$$\begin{aligned} G_h(\mathbf{G},\omega_n) &= \sum_j \frac{V_h^*(\mathbf{G},j)V_h(\mathbf{G}=0,j)}{i\omega_n + \mu_h - \omega_j^h} \\ &= \sum_j \frac{W_h(\mathbf{G},j)}{i\omega_n + \mu_h - \omega_j^h}, \end{aligned} \tag{51}$$

and the density of states (DOS) for the itinerant holes is

$$\begin{aligned} D_h(E) &= -\frac{1}{\pi}\mathrm{Im}G_h(\mathbf{G}=0)\left(\frac{g}{S}\right) \\ &= -\frac{1}{\pi}\mathrm{Im}\sum_j \frac{W_h(\mathbf{G}=0,j)}{E + i\delta - \omega_j^h}\left(\frac{1}{2\pi l_c^2}\right). \end{aligned} \tag{52}$$

The number of bands for the hole density of states should be the same as that for electron but the band gaps should be quantitatively different, since the hole-hole interactions do not play a significant role in the low hole density.

Consider first a single itinerant hole at energy level ω_j^h, from which we calculate the photoluminescence power. Since the hole and the electron have opposite charge (but different effective mass), their lowest Landau level wave functions are just complex conjugates of each other, i.e., $\phi_X^h(\mathbf{r}) = \phi_X^*(\mathbf{r})$. So the luminescence operator can be written as

$$\begin{aligned} \hat{L} &= \int d^2\mathbf{r}\,\psi(\mathbf{r})\psi_h(\mathbf{r}) \\ &= \sum_{X_1X_2}\int d^2\mathbf{r}\,\phi_{X_1}(\mathbf{r})\phi_{X_2}^*(\mathbf{r})a_{X_1}c_{X_2}. \end{aligned} \tag{53}$$

Then the electron-hole recombination process is given approximately by

$$-\langle T_\tau\hat{\mathbf{L}}(\tau)\hat{\mathbf{L}}^\dagger(0)\rangle = -\sum_{X_1X_2}G(X_1,X_2;\tau)G_h(X_1,X_2;\tau). \tag{54}$$

Here, the single-hole Green's function may be written as

$$G_h(\mathbf{G},\tau) = W_h(\mathbf{G},j)e^{-(\omega_j^h - E_0)\tau}, \tag{55}$$

so that the photoluminescense power for single hole at energy level ω_j^h can be written as

$$P_j(\omega) \propto -I_0 \sum_{\mathbf{G}} \mathrm{Im}\left[G(\mathbf{G}, \omega - \omega_j^h) W_h(\mathbf{G}, j)\right]. \quad (56)$$

Since there are many hole states close in energy on the scale of temperature for the itinerant hole, we need to take a thermal average over the different hole states that the electrons may decay into. So the final photoluminescence power in itenerant hole case is given by

$$P(E) = -I_0 \sum_{\mathbf{G}} \sum_{ij} \mathrm{Im} \frac{W_e(\mathbf{G}, i) f_{\mathrm{FD}}(\omega_i^e - \mu_e)}{E + i\delta - \omega_0 - \omega_i^e - \omega_j^h} \times \frac{W_h(\mathbf{G}, j) e^{-\beta\omega_j^h}}{\sum_j W_h(\mathbf{G} = 0, j) e^{-\beta\omega_j^h}}. \quad (57)$$

Here $\omega_0 = \frac{1}{2}\omega_c + \frac{1}{2}\omega_c^h + \Delta$, where ω_c^h is hole cyclotron frequency which is much smaller than that for electron due to the heavier-hole effective mass, and Δ is the conduction-band–valence-band gap.

III. NUMERICAL RESULTS

From the theoretical analysis in the preceding section, we observe that the photoluminescence power just depends on the ground-state electron density $\langle\rho(\mathbf{G})\rangle$, which we can iteratively calculate by directly diagonalizing the matrix B. We can then determine the electron DOS and calculate the photoluminescence power for the localized hole case. For the itinerant hole situation, we can also calculate the hole DOS by directly diagonalizing the matrix B_h, and then calculate the thermal averaged photoluminescence power. In this section, we present our numerical results for the electron ground-state density profile, electron density of states (including DOS for itinerant hole), and the photoluminescence spectra at different temperatures for a magnetic-field-induced Wigner crystal.

As shown in Sec. II, the photoluminescence spectrum is essentially a weighted measure of the density of states of the electron system. As noted earlier, the DOS for a perfect WC is a Hofstadter butterfly. For fractional filling factor $\nu = p/q$, the DOS has q subbands, and at zero temperature, the lowest p bands are filled. We should expect to observe this structure, i.e., p lines for $\nu = p/q$, in the photoluminescence spectrum of an ideal Wigner crystal if we turn off the electron-hole interaction. Presented in Fig. 2 are (a) the density of states and (b) the photoluminescence spectrum for an undisturbed Wigner crystal at $\nu = 2/7$ (Ref. 21) with no electron-hole interaction. We can clearly see that the DOS has seven bands, with only the lowest two occupied at low temperature. As expected, the photoluminescence has two peaks with a splitting identical to that of the DOS. An observation of this behavior in experiments would directly confirm the presence of a Wigner crystal in the system.

Unfortunately, the PL spectrum in Fig. 2 is not experimentally observable for the case of a localized hole, because of the strong interaction of the hole with the electron lattice. We present in Fig. 3 the results for the case of an unscreened hole (e.g., a valence-band hole in a narrow quantum well). We can see, as shown in Fig. 3(b), that there is a single photoluminescence peak which is shifted down in energy from the perfect Wigner crystal case. This structure is best interpreted in terms of the density of states as illustrated in Fig. 3(a), for a periodic electron system with 12 electrons and one localized hole per unit cell. Because of the attractive electron-hole interaction, the WC is deformed in the vicinity of the hole, as shown in Fig. 1(b). The two filled subbands in the density of states break up into three bands, with the lowest-energy peak much smaller in weight but shifted down in energy. The lowest-energy peak corresponds to a bound state of the electrons with the hole, and because this is the only state with a significant overlap with the hole, it dominates the photoluminescence spectrum. To show this, we present in Fig. 4 the electron density profile which corresponds to each energy subband in the DOS. As shown in Fig. 4(a), the lowest-energy peak contains a single electron, localized in the center of the unit cell right above the hole. Since the photoluminescence power

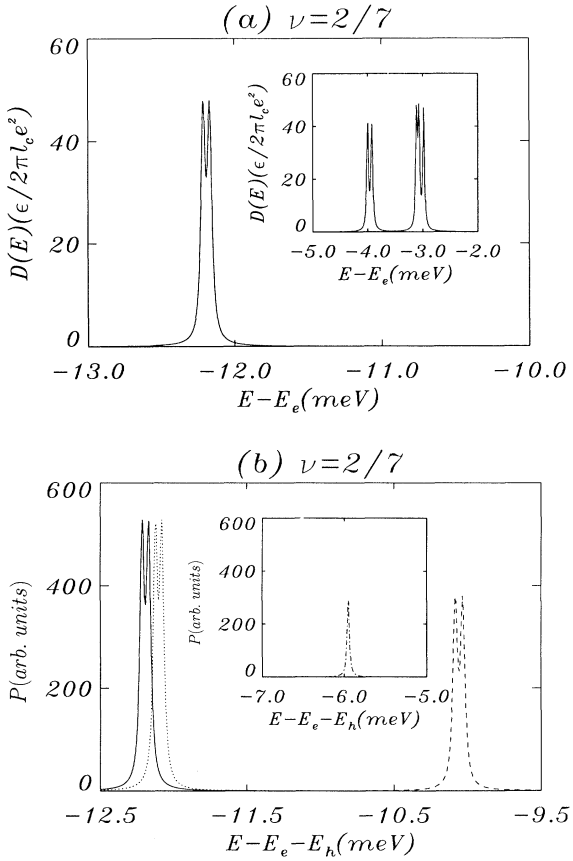

FIG. 2. Electron density of states and PL spectrum for perfect WC with no electron-hole interaction for $\nu = 2/7$. (a) Electron DOS below chemical potential at zero temperature (inset: DOS above chemical potential), where $E_e = \frac{1}{2}\omega_c$; (b) PL spectrum at different temperatures: $T = 0.0045T_{\mathrm{melt}}$ (solid), $T = 0.45T_{\mathrm{melt}}$ (dotted), $T = 0.9T_{\mathrm{melt}}$ (dashed), and $T = 1.12T_{\mathrm{melt}}$ (inset: dash-dotted).

is proportional to the overlap between electron and hole wave functions, this localized electron will certainly overwhelm the PL spectrum. We find that the other peaks in the DOS correspond to sets of electron states that are successively further away from the hole, for increasing energy, as shown in Figs. 4(b) and 4(c). The contribution of these states to the PL is nearly two orders of magnitude smaller than that of the localized electron in the center.

It should be noted that, in most localized hole experiments,[9] the dopant atom is a *neutral* acceptor in its initial state. The interaction of the core hole with the electron gas is then quite weak, leading to a negligible deformation of the WC in its initial state, as shown in Fig. 5(a). However, the *final* state of the dopant is charged, which introduces a strong perturbation in the final state of the WC. Our Hartree-Fock approach does not handle this situation well, as it tends to give qualitatively unrealistic energies when there are strong electron-hole interactions in the final state. It is easy to see, however, that the PL spectrum is still dominated by a single final state, one in which a vacancy is bound to the charged ion, as shown in Fig. 5(b). The PL spectrum should be thus qualitatively the same as described for the case of a strong initial interaction i.e., a single peak will dominate the PL spectrum. We calculate the PL peak energy simply by finding the difference between the Hartree-Fock energies of the initial and final states. The temperature dependence of this PL energy is presented in Fig. 5(c).

Our calculated PL spectrum for a localized hole as the

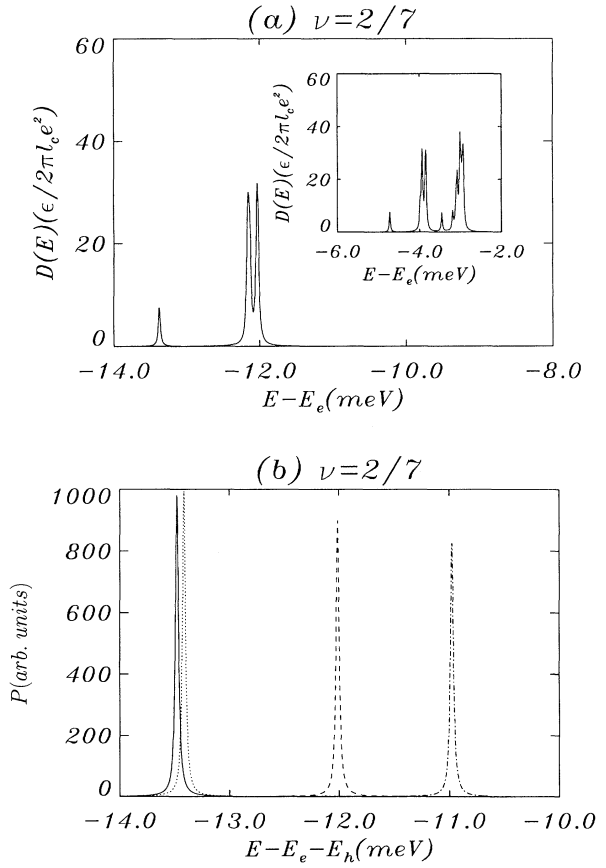

FIG. 3. Electron density of states and PL spectrum for WC in the presence of unscreened interaction between electrons and localized holes for $\nu = 2/7$. (a) Electron DOS below chemical potential at zero temperature (inset: DOS above chemical potential); (b) PL spectrum at different temperatures: $T = 0.0045T_{\rm melt}$ (solid), $T = 0.45T_{\rm melt}$ (dotted), $T = 0.9T_{\rm melt}$ (dashed), and $T = 1.01T_{\rm melt}$ (dash-dotted).

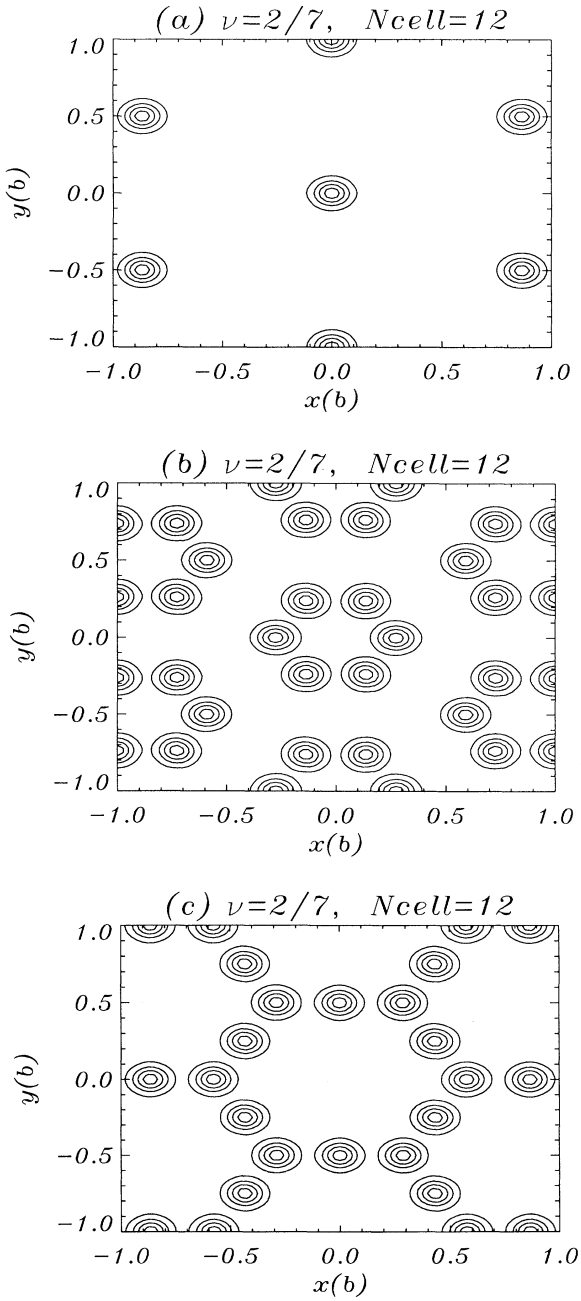

FIG. 4. Electron density profile corresponding to different subbands in DOS: (a) the lowest-energy peak; (b) the second band; (c) the third band.

temperature is raised so as to melt the WC also has very interesting behavior.[22–24] As seen in Fig. 3 (unscreened hole) and Fig. 5 (screened hole), there is an upward shift in the PL peak. The increase in energy corresponds directly to the potential energy lost per electron when the carriers are no longer crystallized. What is remarkable about the shift is that it occurs almost precisely at the melting temperature; there is very little motion just above or below the transition. This is in qualitative agreement with experimental observations, in which two distinguishable lines are observed, with oscillator strength transferring from the lower to the upper one as the temperature is increased. One could interpret

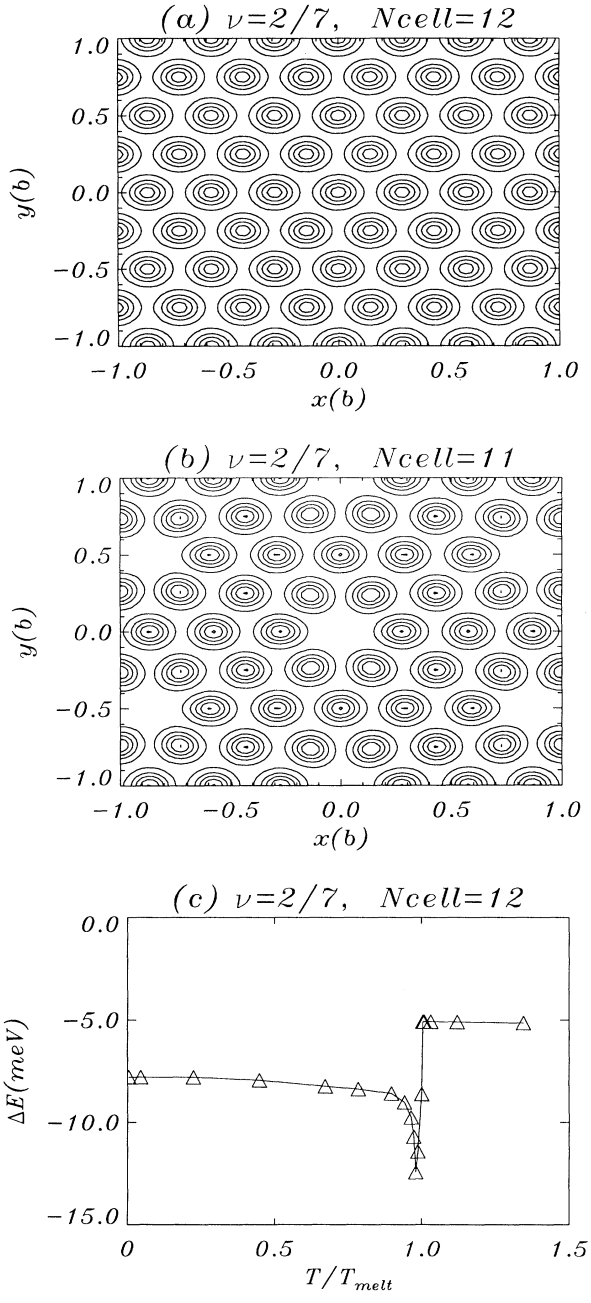

FIG. 5. Results for screened localized hole situation. (a) Electron density profile for the initial state with weak interaction between electrons and a core hole in a neutral acceptor atom; (b) electron density profile for the final state with a vacancy bound to charged acceptor ion; (c) temperature dependence of the PL energy. Note that dip in the PL just below the melting temperature is a finite-size effect.

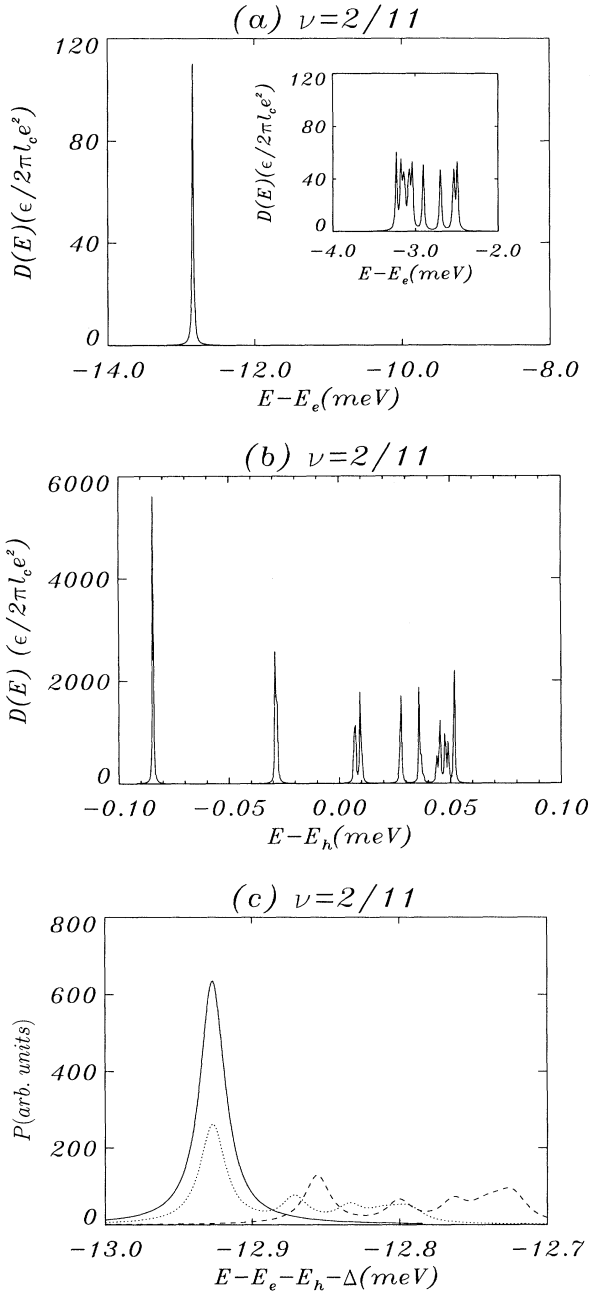

FIG. 6. Results for itinerant hole at $\nu = 2/11$. (a) Electron density of states below chemical potential (inset: DOS above chemical potential), where $E_e = \frac{1}{2}\omega_c$; (b) hole density of states, where $E_h = \frac{1}{2}\omega_c^h$; (c) PL spectrum at different temperatures: $T = 0.0045T_{\rm melt}$ (solid), $T = 0.045T_{\rm melt}$ (dotted), $T = 0.45T_{\rm melt}$ (dashed).

this as finite size domains of the WC with a distribution of melting temperatures, accounting for the continuous transfer of oscillator strength between the two lines. That two such lines are visible in real experiments, rather than a broad continuum PL spectrum, seems consistent with an electrostatic environment for the recombining electrons that is fairly uniform through the sample, indicating that there may be some (substantial) order in the system.

The difficulty of observing local crystalline order directly in PL for the highly localized hole is clearly related to the fact that a single electron dominates the electron-hole recombination. This problem can be alleviated in principle if the hole is not so strongly localized. We thus consider an itinerant hole in the valence band, a geometry which is only very recently being examined in the WC regime.[10] As explained above, electron-hole interactions do not significantly alter the density of states of the Wigner crystal in this case. Typical PL spectrum for this system are shown in Fig. 6(c), for filling fraction $\nu = 2/11$. As shown in Fig. 6(a), the electron density of states has 11 bands with 9 bands above the chemical potential empty, but the splitting between the lowest 2 filled subbands is too small to resolve numerically.[25] This is apparently due to exchange effects. Thus, for the lowest temperatures, one only sees a single peak in the photoluminescence. However, an interesting effect occurs when the temperature is raised slightly (although not nearly enough to melt the crystal): one then finds that structure is introduced in the PL peak. This turns out to be due to the density of states for the hole. The hole also moves in the periodic potential of the electron lattice and the strong magnetic field, and so should be expected to have 11 bands as well, as seen in Fig. 6(b). Since there is no exchange interaction between the hole and the electrons, the hole DOS is qualitatively different from that of the electrons. Specifically, the gap between the lowest two bands of the hole is much larger than that of the electrons, but much smaller than the band gap between occupied and unoccupied electron states of the WC. So if we increase the temperature moderately so as to allow some non-negligible probability for the hole to occupy the higher bands, but the electrons remain in the lowest two bands, each hole subband that has a significant probability of occupation will add a new line to the PL spectrum. Once again, observation of this effect would constitute direct confirmation of crystalline order in the 2DEG. We believe that, with increasing sample quality, this effect should be observable in wider-well geometries.

IV. CONCLUSION

In summary, we have developed a theory of photoluminescence for the WC in a strong magnetic field using the time-dependent Hartree-Fock approximation. We find that the PL spectrum is a weighted measure of the DOS of the electron system. One can use PL to unambiguously demonstrate the presence of a WC, by observing a gap structure associated with the unique energy spectrum of an electron in a periodic potential and a magnetic field. We show that electron-hole interactions arising from a localized hole (both screened and unscreened) tend to remove the Hofstadter structure from the PL spectrum. Instead, the PL is dominated by a single peak, arising from a single electron localized in the vicinity of an unscreened hole. Similarly, for the screened hole, a vacancy bound to the charged acceptor ion is the only final state significantly contibuting to the PL, resulting again in a single line. The behavior of the PL spectrum for the WC in the case of a localized hole at finite temperature was also investigated. We found an upward shift in PL energy as we approach melting point of the WC which qualitatively agrees with the experiment. We also argued that in an itinerant hole experiment, the gap structure will be observed by raising the temperature because the hole itself has a Hofstadter density of states, due to the periodic potential provided by the electron WC and the magnetic field. We believe that, with improved sample quality, itinerant hole PL experiments should offer the best opportunity to observe this type of structure, which is a direct consequence of the presence of a WC.

Finally, it is important to note that any real sample inevitably has disorder, so that one should expect these systems to form domains separated by grain boundaries (provided the disorder is not strong enough to completely eliminate local crystalline order). The effects of this disorder most likely would be to fill in the gaps in the density of states that are associated with the Hofstadter butterfly. Clearly, one needs a very high-quality sample to see direct indications of crystal order in the PL.

ACKNOWLEDGMENTS

The authors thank the University of Kentucky Center for Computational Sciences for providing computer time. This work is supported by the National Science Foundation through Grants Nos. DMR 92-02255 (H.A.F.) and 91-23577 (D.Z.L. and S.D.S.).

[1] E.P. Wigner, Phys. Rev. **46**, 1002 (1934).
[2] B. Tanatar and D.M. Ceperley, Phys. Rev. B **39**, 5005 (1989).
[3] C.C. Grimes and G. Adams, Phys. Rev. Lett. **42**, 795 (1979).
[4] Some recent experimental work has suggested the possibility that the WC is observable at zero field in MOSFET's. See V.M. Pudalov, M. D'Iorio, S.V. Kravchenko, and J.W. Campbell, Phys. Rev. Lett. **70**, 1866 (1993).
[5] E.Y. Andrei, G. Deville, D.C. Glattli, F.I.B. Williams, E. Paris, and B. Etienne, Phys. Rev. Lett. **60**, 2765 (1988); F.I.B. Williams *et al.*, *ibid.* **66**, 3285 (1991).
[6] M.A. Paalanen, R.L. Willett, P.B. Littlewood, K.W. West, L.N. Pfeiffer, and D.J. Bishop, Phys. Rev. B **45**, 11 342 (1992).
[7] V.J. Goldman, M. Santos, M. Shayegan, and J.E. Cunningham, Phys. Rev. Lett. **65**, 2189 (1990); H.W. Jiang, R.L. Willett, H.L. Stormer, D.C. Tsui, L.N. Pfeiffer, and K.W.

West, *ibid.* **65**, 633 (1990); Y.P. Li, T. Sajoto, L.W. Engel, D.C. Tsui, and M. Shayegan, *ibid.* **67**, 1630 (1991).

[8]M. Besson, E. Gornick, C.M. Engelhardt, and G. Weimann, Semicond. Sci. Technol. **7**, 1274 (1992).

[9]H. Buhmann *et al.*, Phys. Rev. Lett. **66**, 926 (1991); I.V. Kukushkin *et al.*, Phys. Rev. B **45**, 4532 (1992).

[10]E.M. Goldys *et al.*, Phys. Rev. B **46**, 7957 (1992); R.G. Clark, Phys. Scr. **T39**, 45 (1991), and references therein.

[11]A mean-field approach cannot account for correlation effects associated with the Fermi-edge singularity encountered in PL in metals. However, since the WC has no Fermi surface, this is not a problem for our present purpose.

[12]D. Hofstadter, Phys. Rev. B **14**, 2239 (1976).

[13]H.A. Fertig, D.Z. Liu, and S. Das Sarma, Phys. Rev. Lett. **70**, 1545 (1993).

[14]L. Bonsall and A.A. Maradudin, Phys. Rev. B **15**, 1959 (1977).

[15]R. Côté and A.H. MacDonald, Phys. Rev. Lett. **65**, 2662 (1990); Phys. Rev. B **44**, 8759 (1991).

[16]G. Mahan, *Many-Particle Physics* (Plenum Press, New York, 1983).

[17]This exchange term is the band-gap renormalization due to electron-hole interaction, which vanishes in the thermodynamic limit $S^{-1} \to 0$ under TDHFA.

[18]H.A. Fertig, R. Côté, A.H. MacDonald, and S. Das Sarma, Phys. Rev. Lett. **69**, 816 (1992).

[19]However, the residues of the poles are not the same as for the Green's function. The residues are determined by the overlaps of the mean-field single-particle electron wave functions with the hole wave function. It is thus appropriate to think of R as a weighted Green's function. Since $P'(\omega)$ involves the imaginary part of $\mathrm{R}(\omega)$, our final result takes the form of a weighted density of states.

[20]Because we have taken the limit $E_0 \to \infty$, we always consider situations in which the inital state of the hole is occupied with probability 1; we thus do not consider excitonic correlations between the electrons and the hole, which would enter here as a nonzero expectation value $\langle\psi(0)\psi_h(0)\rangle$, for a hole tightly bound to a site at the origin. This should be valid so long as the hole is not too close to the electron gas on the scale of the magnetic length, as is the case in most experiments. See A.H. MacDonald, E.H. Rezayi, and D. Keller, Phys. Rev. Lett. **68**, 1939 (1992)

[21]The filling $\nu = 2/7$ is higher than the fillings at which the WC is believed to be the ground state of the system. However, our results should be qualitatively the same as for lower fillings, and the use of a larger ν allows us to obtain better numerical accuracy. Results for an experimentally relevant filling ($\nu = 2/11$) for the itinerant hole case are given in Fig. 6.

[22]Because of the mean-field nature of the Hartree-Fock approximation, our calculation does not describe the melting transition when the magnetic field is adjusted so that the electrons melt into a fractional quantum Hall fluid. The data for this melting transition are also quite different than the temperature-driven melting transition, suggesting that the physics of the two types of transitions is quite different. In this work, we address only temperature-driven melting.

[23]The Hartree-Fock approach to melting cannot account for fluctuation effects that might lead, for example, to a Kosterlitz-Thouless transition. However, since the PL for a core hole is a probe of *local* electron structure, we believe our calculation gives the correct qualitative behavior.

[24]Excited phonon modes at finite temperatures strongly renormalize the electron density modulations, leading to lower melting temperatures than those calculated in the TDHFA, as well as a broadening of the peak structures in all our figures. However, we do not expect this to affect any of our qualitative conclusions.

[25]D. Yoshioka and P.A. Lee, Phys. Rev. B **27**, 4986 (1983), found a similarly small splitting at this filling.